Heliyon

Received:
19 May 2017
Revised:
26 May 2017
Accepted:
11 September 2017

Cite as: Yoshifumi Iwagami, Sarah Casulli, Katsuya Nagaoka, Miran Kim, Rolf I. Carlson, Kosuke Ogawa, Michael S. Lebowitz, Steve Fuller, Biswajit Biswas, Solomon Stewart, Xiaoqun Dong, Hossein Ghanbari, Jack R. Wands. Lambda phage-based vaccine induces antitumor immunity in hepatocellular carcinoma. Heliyon 3 (2017) e00407.
doi: 10.1016/j.heliyon.2017.e00407

Lambda phage-based vaccine induces antitumor immunity in hepatocellular carcinoma

Yoshifumi Iwagami [a,1], Sarah Casulli [a,1], Katsuya Nagaoka [a], Miran Kim [a], Rolf I. Carlson [a], Kosuke Ogawa [a], Michael S. Lebowitz [b], Steve Fuller [b], Biswajit Biswas [b], Solomon Stewart [b], Xiaoqun Dong [c], Hossein Ghanbari [b], Jack R. Wands [a,*]

[a] *Division of Gastroenterology and Liver Research Center, Warren Alpert Medical School of Brown University and Rhode Island Hospital, Providence, RI, 02903, USA*

[b] *Panacea Pharmaceuticals, Gaithersburg, MD, 20877, USA*

[c] *Department of Internal Medicine, College of Medicine, University of Oklahoma Health Sciences Center, Oklahoma City, OK, 73104, USA*

* Corresponding author at:
E-mail address: Jack_Wands_MD@Brown.edu (J.R. Wands).

[1] These authors contributed equally to this work.

Abstract

Background and aims: Hepatocellular carcinoma (HCC) is a difficult to treat tumor with a poor prognosis. Aspartate β-hydroxylase (ASPH) is a highly conserved enzyme overexpressed on the cell surface of both murine and human HCC cells.

Methods: We evaluated therapeutic effects of nanoparticle lambda (λ) phage vaccine constructs against ASPH expressing murine liver tumors. Mice were immunized before and after subcutaneous implantation of a syngeneic BNL HCC cell line. Antitumor actively was assessed by generation of antigen specific cellular immune responses and the identification of tumor infiltrating lymphocytes.

Results: Prophylactic and therapeutic immunization significantly delayed HCC growth and progression. ASPH-antigen specific CD4+ and CD8+ lymphocytes were identified in the spleen of tumor bearing mice and cytotoxicity was directed against ASPH expressing BNL HCC cells. Furthermore, vaccination generated antigen specific Th1 and Th2 cytokine secretion by immune cells. There was

http://dx.doi.org/10.1016/j.heliyon.2017.e00407

widespread necrosis with infiltration of CD3+ and CD8+ T cells in HCC tumors of λ phage vaccinated mice compared to controls. Moreover, further confirmation of anti-tumor effects on ASPH expressing tumor cell growth were obtained in another murine syngeneic vaccine model with pulmonary metastases.

Conclusions: These observations suggest that ASPH may serve as a highly antigenic target for immunotherapy.

Keywords: Vaccines, Cancer research, Oncology, Medicine, Immunology, Cell biology

1. Introduction

Hepatocellular carcinoma (HCC) is one of the most common malignancies and the second leading cause of cancer mortality worldwide [1]. Successful surgical resection helps improve the overall survival; however, the long-term prognosis is dismal due to the high frequency of recurrence (50–60%) in the remnant liver [2]. Furthermore, only 10–15% of patients are suitable for surgical resection at diagnosis and there are very limited therapeutic options for unresectable HCC [3]. In advanced stage disease, the multi-targeted kinase inhibitor, sorafenib offers an overall survival benefit of 2.8 months (without significant difference in the median time to symptomatic progression) [4]. It is noteworthy that no beneficial effect of this drug on survival has yet been observed in the adjuvant setting [5, 6]. Therefore, there is a need to develop novel and effective therapeutic approaches to prevent disease reoccurrence and improve clinical outcome of individuals with established disease.

Aspartate β-hydroxylase (ASPH) is a highly conserved type II transmembrane protein, composed of 758 amino acids with a molecular weight of ~86-kDa, that belongs to the α-ketoglutarate-dependent dioxygenase family [7]. The ASPH was originally described as being overexpressed in HCC and cholangiocarcinoma (CCC) [8]. Interestingly, ASPH has been detected in 85–90% of human HCC tumors, but not in dysplastic nodules and normal liver [9]. In general, ASPH expression is very low or negligible in normal adult tissues except the placenta [8]. Moreover, ASPH is expressed on the surface of tumor cells where both N-terminal sequences and the catalytic site located in the C-terminal region have been shown to be accessible antigens to the immune system. ASPH contains numerous immunogenic peptides (epitopes) that are presented to major histocompatibility (MHC) class I and II molecules, which will subsequently induce ASPH epitope-specific CD4+ and CD8+ T cell responses in both human and animal models of HCC [10].

Bacteriophage display can achieve favorable peptide presentation to the immune system [11]. Bacteriophage lambda (λ) has been shown to stably display fusion proteins on its capsid protein, with copious copies of these antigenic peptides

http://dx.doi.org/10.1016/j.heliyon.2017.e00407

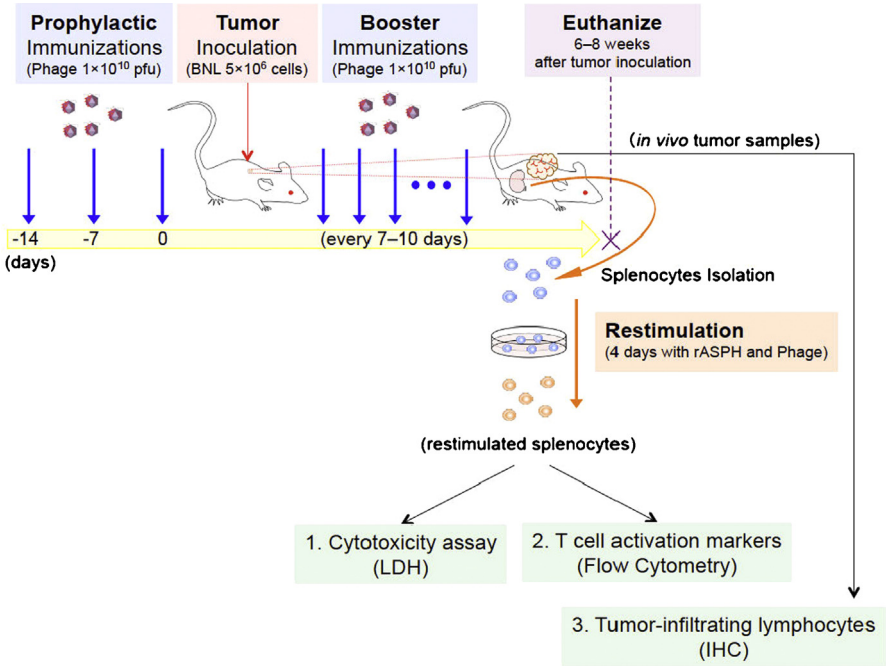

Fig. 1. Experimental overview. Mice were immunized by injecting 1×10^{10} pfu of Phage particles. Prophylactic immunizations were injected 3 times on Day − 14, Day − 7 and Day 0. Booster immunizations were continuously injected every 7–10 days after tumor inoculation (5×10^6 BNL cells). Six to eight weeks after tumor inoculation, mice were euthanized. After re-stimulation of splenocytes with recombinant ASPH protein (rASPH) and λ3 phage, cytotoxicity assays and flow cytometric analysis were performed, and tumor samples were collected for immunohistochemistry and demonstration of T cell infiltration.

represented that may be 2–3 orders of magnitude higher than other phage display vectors [12]. In this study, we targeted an ASPH expressing murine HCC cell line and confirmed findings with another murine tumor induced by 4T1 ASPH expressing cells in an attempt to develop an immunotherapeutic approach for HCC as shown in Fig. 1.

2. Results

2.1. Construction of λ phage nanoparticles expressing human ASPH derived proteins

The ASPH is highly homologous between the human and murine orthologs. For example, overall 84.4% of the amino acids are conserved when comparing human to murine ASPH sequence; this similarity is particularly prominent in the C-terminal region of the λ3 vaccine construct where they are 99.5% identical (Fig. 2A). In addition, human leukocyte (HLA) class I and II peptides are highly represented in this region of the ASPH molecule [10]. It was also confirmed by

http://dx.doi.org/10.1016/j.heliyon.2017.e00407

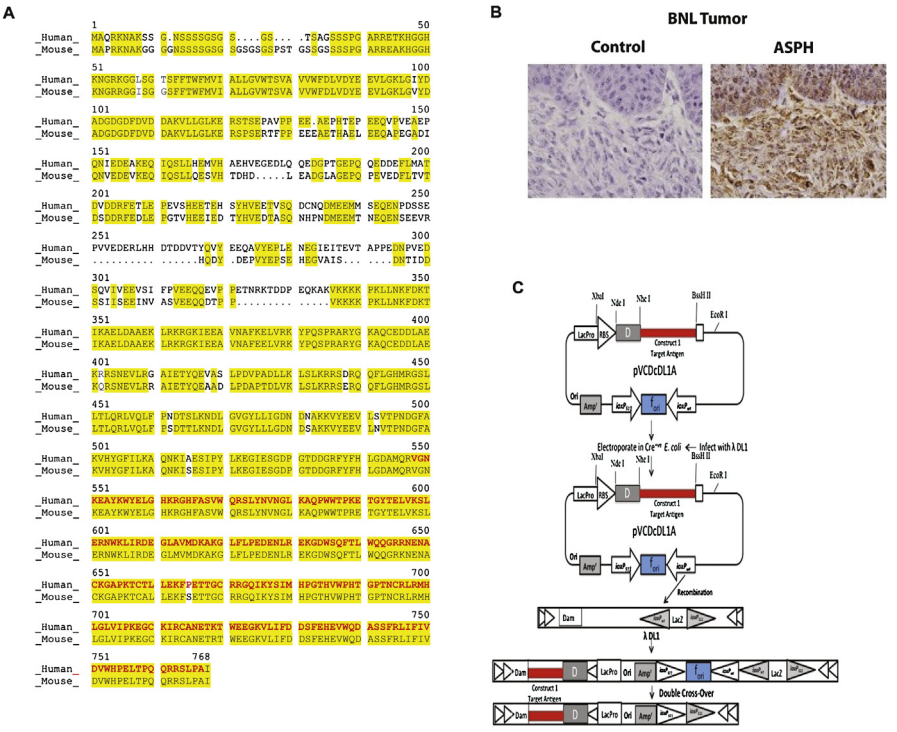

Fig. 2. Characteristics of λ phage particles expressing human ASPH protein. (A) The map of the human ASPH sequence containing 758 amino acids (NCBI accession No. NP_004309) compared to the structural map of the murine ASPH sequence containing 725 amino acids (NCBI accession No. NP_001171320). The yellow highlighted sequences represent the homology between mice and humans. The red sequences shows the murine verses human sequences in the λ3 vaccine construct. (B) Representative example of high level ASPH expression in murine BNL derived HCC tumor by IHC using a rabbit polyclonal antibody prepared against human recombinant ASPH protein [18]. The control was rabbit IgG employed as a primary antibody (1000×). (C) Homologous recombination of donor plasmid pVCDcDL3 with recipient phage vector λ-DL1. Only part of the lambda genes are shown. The unique Nhe I and BssH II sites were used to clone ASPH segments into the pVCDcDL1A plasmid. Generated recombinant phages were designated as ASPH construct λ3 which contained the inserted ASPH fragments. The inserts were fused with the GpD capsid protein gene of the λ phage to produce GpD-ASPH fusion construct located on the λ head. Only the diagram of the λ1 construct is shown here. The maps are not drawn to scale.

immunohistochemistry (IHC) that the ASPH protein was highly expressed in the murine BNL HCC cell line as shown in Fig. 2B.

In this context of high homology between murine and human ASPH, we designed, developed and produced λ phage vaccine contructs displaying ASPH protein fragments on their surfaces for subsequent immunization. The λ phage has a number of gpD head proteins on its surface. A segment of the human ASPH protein fused to gpD is employed. The λ phage particles expressing human ASPH peptides were designated as λ1 and λ3 as they include sequences derived from the N-terminal region (1/3 of the protein sequence) and from the extracellular

http://dx.doi.org/10.1016/j.heliyon.2017.e00407

C-terminal third of human ASPH protein, respectively. The target antigens were inserted into a donor plasmid vector, and Escherichia coli (*E. coli)* were transfected and subsequently infected with the recipient λ phages. Recombination occurred *in vivo* and the target antigen was displayed and fused to the phage gpD protein as shown in Fig. 2C. The bacteriophage vaccine constructs were isolated and purified using tangential flow filtration, PEG precipitation and dialysis. The bacteriophage vaccines were rendered noninfectious by ultraviolet irradiation.

It has been previously demonstrated that human ASPH loaded dendritic cells (DCs) induced epitope-specific T cell responses in patients with HCC [10]. Fifteen MHC class-II restricted peptides had been predicted using an immunoinformatics analysis. [13] Two peptides were found to reside in the N-terminal domain (λ1), and 6 were located in the C-terminal region of ASPH in the λ3 construct. Similarly, 30 MHC class-I restricted ASPH epitopes were predicted as well [10]. We focused the vaccine studies using both the λ1 and λ3 phage constructs where empty phage and saline injections served as negative controls.

2.2. Effect of λ phage immunization on HCC growth in vivo

Alterations of tumor growth and progression were observed using 3 prophylactic immunizations with λ1 and λ3 phage constructs, and subsequent subcutaneous implantation of BNL tumor cells, which was then followed by booster immunization administered every 7–10 days. With respect to reduction in tumor growth rate and progression, there were significant differences between the control (empty) phage and λ1 immunized animals (Fig. 3). Similar differences ($p < 0.001$) were observed with λ3 vaccinated animals as well (Fig. 4). An *in vitro* cytotoxity assay was performed using splenocytes derived from immunized mice with λ3 phage to demonstrate generation of ASPH-specific cytotoxity using ASPH expressing BNL HCC cells as the target as shown in Fig. 4. There were significant differences in target cell lysis between the control splenocytes and those derived from the λ3 immunized mice (Fig. 4B). Thus, immunization with both λ1 and λ3 phage before inoculation of BNL cells followed by a boost every 7–10 days efficiently inhibited tumor growth and prolonged overall survival compared to controls (Fig. 4A and C).

2.3. Generation of cellular immune responses to ASPH

Splenocytes derived from λ3 phage-immunized mice were re-stimulated with recombinant ASPH protein (rASPH) and λ3 phage particles, which promoted the activation of CD4+ cells to co-express CD154 and secrete IFNγ (Fig. 5A). In addition, CD8+ cells were found to co-expressed CD137, and secreted IFNγ as well (Fig. 5B). To further evaluate the characteristics of cellular immune response to ASPH, we measured secretion of IL-2, IL-4, IL-6, IL-10, IFN-γ and TNF-α by

http://dx.doi.org/10.1016/j.heliyon.2017.e00407

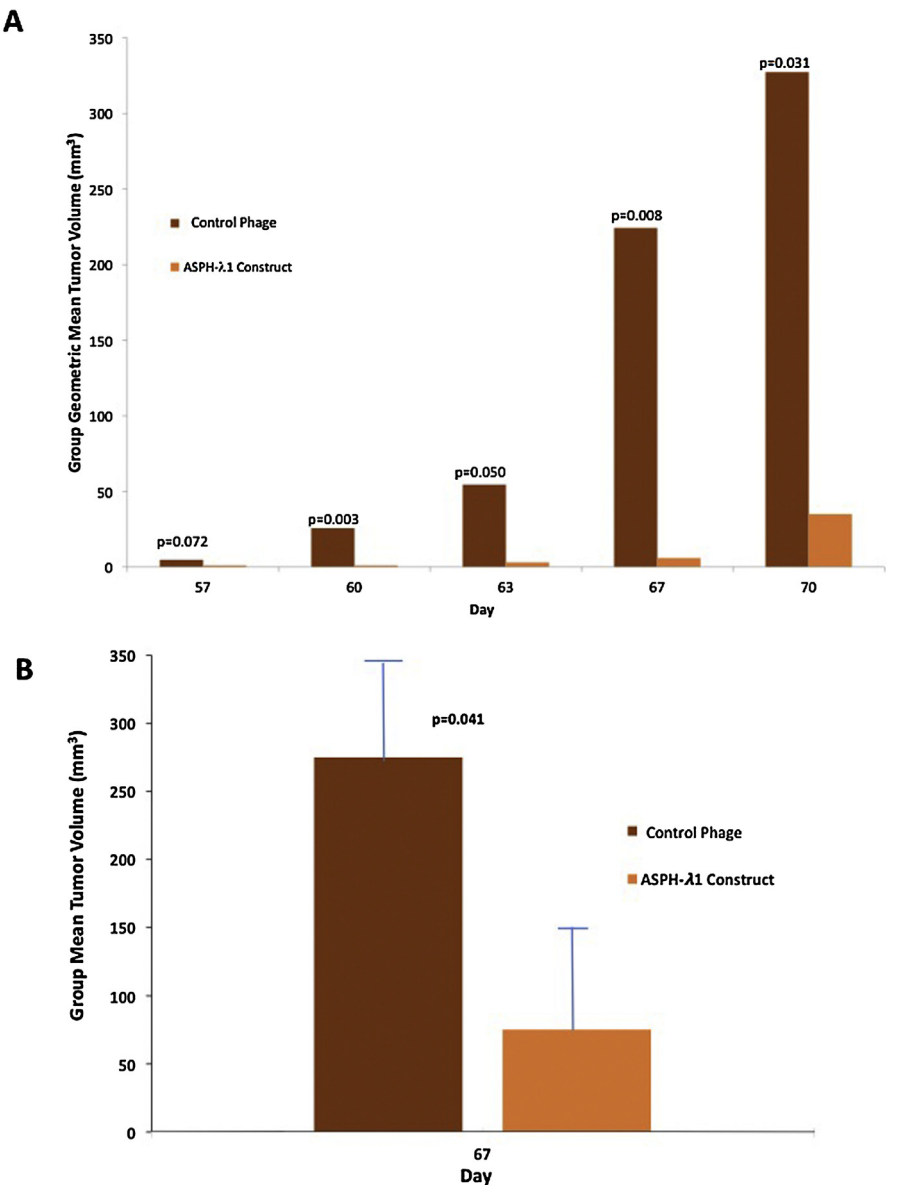

Fig. 3. Anti-tumor effect of vaccination with the ASPH-λ1 construct compared to the control parental phage on the growth of murine BNL HCC cells in Balb/c mice (N = 5). There was significant reduction in sub-cutaneous tumor growth following vaccination with the ASPH-λ1 phage construct compared to the parental phage lacking the ASPH sequences. (A) represents the group geometric mean tumor volume followed over 70 days of observation. (B) anti-tumor effects of the λ1 vaccine construct on group mean tumor volume at day 67 ($p < 0.041$).

splenocytes derived from immunized mice by ELISA. As shown in Fig. 6, the levels of Th1 (IFN-γ and TNF-α) and Th2 (IL-4, IL-6 and IL-10) cytokine levels in the culture supernatants were higher than those found in the splenocytes derived from control mice. Interestingly, this λ3 phage vaccine construct elicited a mixed Th1 and Th2 immune response since the production of IL-2 was found to be significantly lower.

http://dx.doi.org/10.1016/j.heliyon.2017.e00407

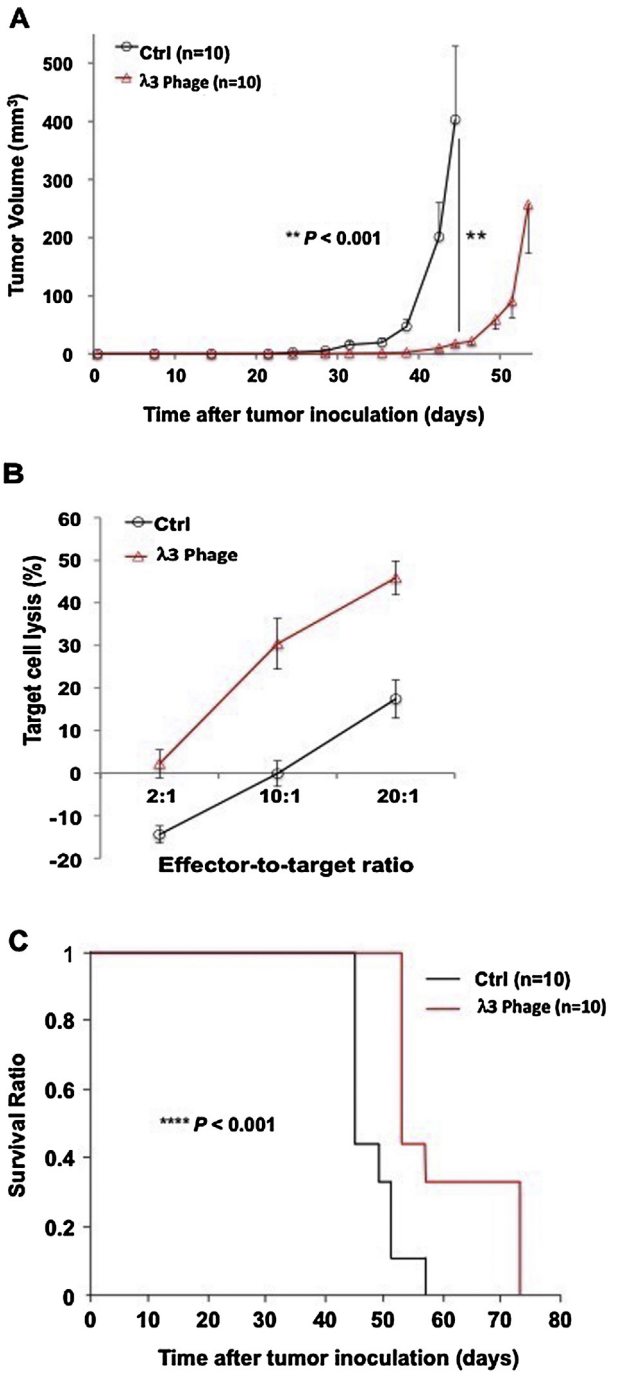

Fig. 4. Antitumor effects generated by immunization with phage particles expressing human ASPH peptides. (A) Growth rate of HCC tumors in animals receiving 3 prophylactic immunizations with λ3 phage followed by booster immunizations every 7–10 days. Mean volume of BNL derived HCC tumors are shown (n = 10). This experiment was repeated 3 times with similar results. (B) Results of *in vitro* cytotoxicity assays against BNL, a syngeneic murine HCC cell line used as the target. Splenocytes were derived from mice immunized 5-times with the λ3 phage. Mean target cell lyses values were calculated from triplicate cultures; 3 independent experiments were performed with similar observations. (C) Kaplan-Meier survival curves of the same animals shown in (c) (n = 10). Results were presented as the mean ± SEM. $^{**}P < 0.01$, $^{****}P < 0.001$.

http://dx.doi.org/10.1016/j.heliyon.2017.e00407

2.4. Immunization with λ3 phage vaccine constructs induced tumor-infiltrating lymphocytes

The gross appearance and H&E staining of BNL HCC xenograft tumors revealed striking differences when comparing the λ3 phage immunized mice to the controls. There were massive areas of necrosis and lymphocytic infiltration in tumors derived from λ3 vaccinated mice (Fig. 7A). The ASPH expression remained detectable on residual tumor cells derived from λ3 immunized mice (Fig. 7B; middle panel). Tumor-infiltrating CD3+ T cells were substantially increased in λ3 immunized mice (Fig. 7B). The phenotypes of tumor-infiltrating lymphocytes using anti-CD8 and anti-CD45 antibodies were examined. (Figs. 7 C and 8). There was a significant increase in both CD8+ and CD45+ cells in tumors derived from λ3 immunized mice.

To further validate and extend these observations, we employed another syngeneic murine model of pulmonary metastasis [14] using 4T1 breast carcinoma cells injected into the 4th mammary gland. These cells also overexpress ASPH by IHC as shown in Fig. 9A. Animals vaccinated with both λ1 and λ3 phage constructs demonstrated enhanced survival (Fig. 9B). Indeed, all 8 mice immunized with λ3 construct survived over the observation period whereas 7 of 8 others immunized with control phage had to be sacrificed due to large primary tumor burden in the breast at the end of the study ($p < 0.001$). More important, immunization with the λ1 phage construct strikingly reduced pulmonary metastasis compared to the empty phage control (Fig. 9C).

3. Discussion

These studies suggest that immunization with two different λ phage constructs representing N and C-terminal sequences of ASPH have anti-tumor effects on the growth and progression of liver cancer generated by BNL HCC cells in a syngeneic murine tumor model. Results were confirmed *in vivo* by another ASPH expressing 4T1 breast cancer cell line that grows rapidly in the mammary gland and subsequently metastasizes to the lung; immunization with the phage vaccine constructs improved overall survival and reduced pulmonary metastasis. Phage vaccination also generated antigen specific $CD4^+$ and $CD8^+$ activity *in vitro* and led to tumor infiltration with effector T cells leading to widespread necrosis. These findings suggest that ASPH may be an attractive target for an immunotherapeutic vaccine approach.

It has been observed that ASPH catalyzes the hydroxylation of β carbons in aspartyl and asparaginyl residues found in many signaling molecules [7, 8, 15, 16]. Its enzymatic activity depends on the presence of ferric iron and α-ketoglutarate as well as substrates that contain epidermal growth factor (EGF) like repeats [15]. During oncogenesis, the protein translocates to the cell surface leading to N and

http://dx.doi.org/10.1016/j.heliyon.2017.e00407

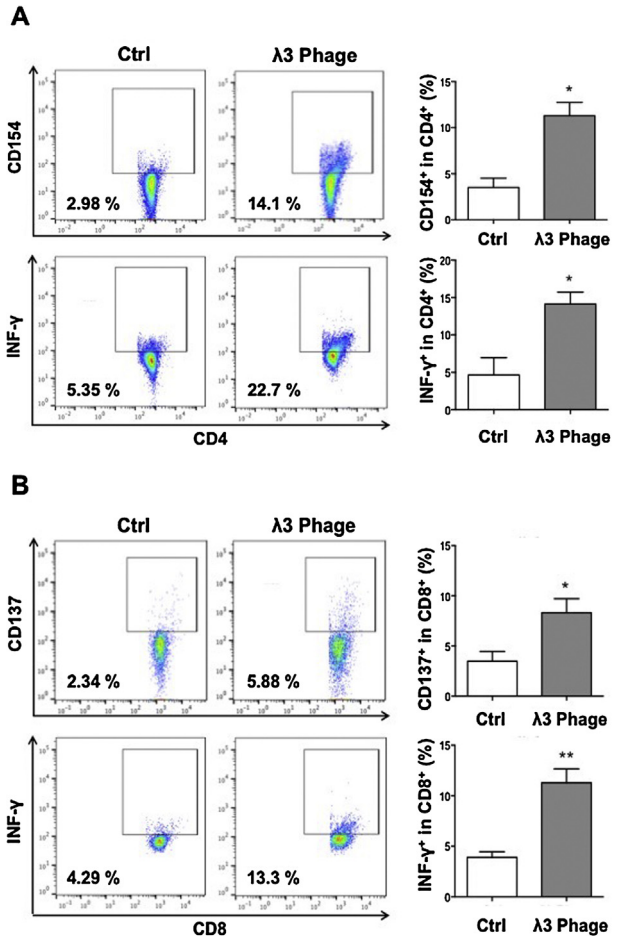

Fig. 5. Generation of antigen specific CD4+ and CD8+ T cells induced by immunization with λ3 phage particles. Specific activation of T cells was evaluated using splenocytes derived from the mice bearing BNL tumors following ASPH restimulation (Fig. 1). Splenocytes were restimulated with 0.5 μg/ml rASPH and 2×10^8 pfu/ml phage particles in combination for 4 days. (A) ASPH-specific activation of CD4+ T cells as measured by expression of CD154 and IFNγ (left panel). The percent of CD154 and IFNγ positive cells in this population are shown in the right panel. (B) ASPH specific activation of CD8+ T cells as shown by the expression of CD137 and IFNγ (left panel). The percent of CD137 and IFNγ positive cells in this cell population are shown in the right panel. Bar graphs represent the means ± SEM. *$p < 0.05$, **$p < 0.01$.

C-terminal regions exposed to the extracellular environment and its functions could be modulated by the host immune responses. More important, the presence of antigenic epitopes that reside on these regions can efficiently stimulate T-cell responses specific to tumor cells harboring ASPH [10]. Previous studies have established that ASPH is a viable target for immunotherapy using a dendritic cell (DC) microparticle vaccine in syngeneic animal models of HCC and cholangiocarcinoma which has some similarities to the λ phage vaccine constructs presented here [17, 18]. The ASPH is highly conserved during mammalian evolution. It is expressed in the embryo during development, but at birth the gene is silenced only

http://dx.doi.org/10.1016/j.heliyon.2017.e00407

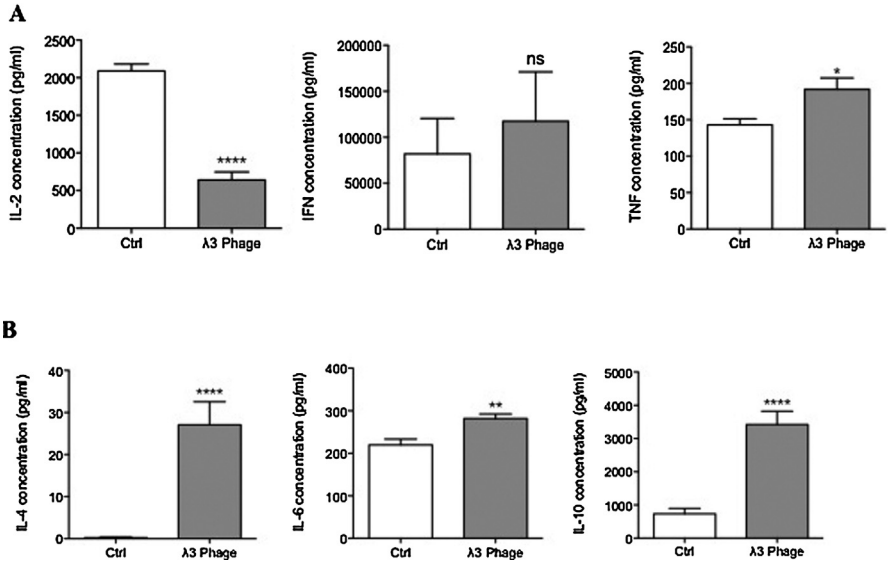

Fig. 6. Immunization with λ3 phage particles induce Th1 and Th2- cytokines responses. (A) Protein levels of Th1-type cytokines IL-2 (left panel), IFN-γ (middle panel) and TNF-α (right panel) in cell culture supernatants were measured by ELISA in λ3 immunized mice (N = 10). (B) Levels of Th2-type cytokines IL-4 (left panel), IL-6 (middle panel) and IL-10 (right panel) in cell culture supernatants as determined by ELISA in λ3 immunized mice (N = 10). *$p < 0.05$, **$p < 0.01$, ****$p < 0.0001$.

to be reactivated during transition of normal cells to the malignant phenotype [8, 9].

ASPH directly contributes to oncogenesis since its overexpression stimulates tumor cell proliferation, migration, and invasion [9, 13, 19] and it was of interest to find the phage vaccination substantially reduced pulmonary metastasis in the 4T1 breast cancer murine model. Expression of ASPH in normal tissues is generally low or negligible except for the placenta, a highly invasive tissue, where gene and protein expression approach the levels found in many human HCC tumors. In this regard, IHC staining for protein expression and RT-PCR for mRNA upregulation have revealed that approximately 85% of hepatitis C virus (HCV) and hepatitis B virus (HBV) related HCC, as well as 95% of cholangiocarcinomas exhibit upregulation of the ASPH gene [9, 17, 18, 20, 21, 22].

ASPH has been found to exert its biologic effects during oncogenesis by the following mechanisms: 1) promotes activation of the Notch signaling cascade; 2) inhibits apoptosis through caspase 3 cleavage; 3) enhances cell proliferation via phosphorylation of RB1; 4) delays cell senescence; and 5) generates cancer stem cells [21, 22, 23]. The transcriptional regulation of ASPH is controlled by well-known signaling cascades such as IN/IRS-1/Raf/Ras/MAP/Erk, IN/IRS-1/PI3 K/AKT and WNT/β-catenin signaling [20, 24]. In this context, ASPH becomes a key molecue that links upstream growth factor signaling pathways to Notch activation and subsequent downstream expression of Notch target genes to participate in

http://dx.doi.org/10.1016/j.heliyon.2017.e00407

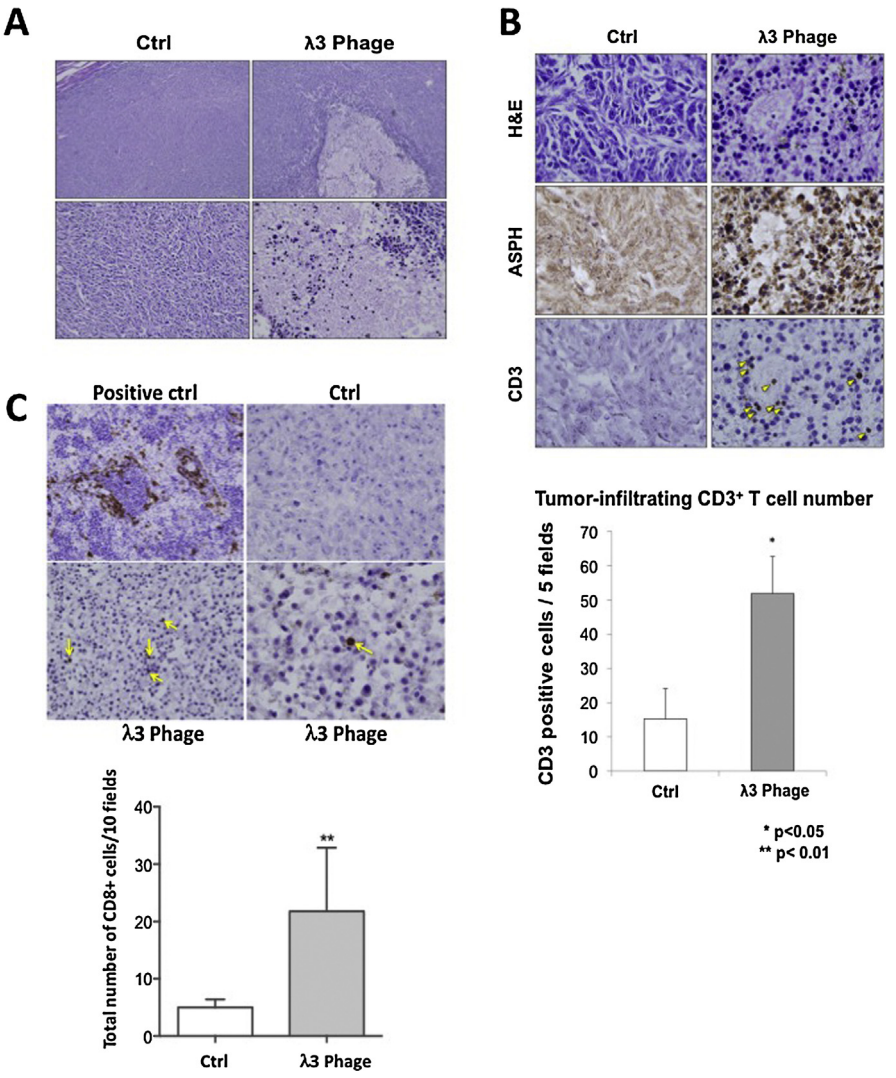

Fig. 7. Immunization with λ 3 phage containing human ASPH mediates tumor necrosis. (A) Histopathological features of excised tumors derived from the immunized mice and controls bearing BNL induced HCC tumors. Representative photographs of hematoxylin and eosin (H&E) staining (top: 100×, bottom: 400×) showing massive necrosis and mononuclear cell infiltration of BNL generated HCC tumors in the λ3 phage immunized mice compared to control. (B) Mononuclear tumor-infiltrating cells were numerous in vaccinated mice by H&E staining (top panel). Tumor cells from both control and immunized mice still expressed ASPH (middle panel). Infiltrating mononuclear cells were derived in part from CD3+ cells (yellow arrows; 400×). There were very few CD3+ cells in the tumors derived from controls. Tumor-infiltrating mononuclear cells were quantified and expressed as average number of CD3+ cells in 5 high-powered fields (bottom panel; 400×). (C) The number of CD8+ cells infiltrating the tumors of λ3 vaccinated mice (yellow arrows) are presented compared to controls. The CD8+ cells were quantitated in 10 high powered fields (1000×) and tumors derived from immunized mice were compared to controls. The spleen was used as the positive control for CD8+ cells. Bar graphs represented the mean ± SEM. *$P < 0.05$. **$P < 0.01$.

http://dx.doi.org/10.1016/j.heliyon.2017.e00407

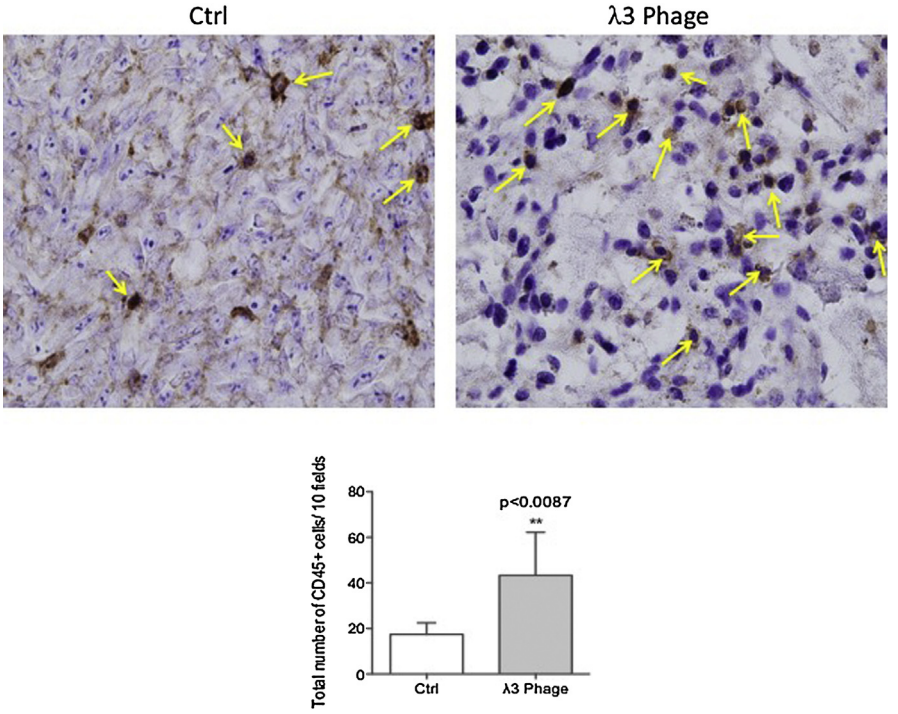

Fig. 8. Determination of CD45+ mononuclear cells infiltrating tumors derived from λ3 phage vaccinated mice. Numerous CD45+ mononuclear cells had infiltrated tumors derived from λ3 phage vaccinated animals (right panel) as compared to the control (left panel). There was a significant difference in the quantity of CD45+ cells between the two representative tumors (**$p < 0.01$). The bar graphs depicted the quantitative data obtained from multiple sections derived from three control and three λ3 phage vaccinated mice with respect to CD45+ cell infiltration into the tumor parenchyma. The total number of CD45+ cells were determined at 1000× from 10 high powered fields in each tumor section.

hepatic oncogenesis. There are also post-translational modifications of ASPH in tumor cells by GSK3β via phosphorylation of the motifs located in the N-terminal region of the protein [25].

It is of interest that activation of IN/IGF1/IRS1 mediated pathways, as well as WNT/β-catenin and ASPH/Notch signaling cascades has been shown to be necessary and sufficient for promoting transformation of the normal liver to a malignant phenotype in a double transgenic murine model [26]. Therefore, inhibition of the expression and function of this putative tumor related target protein could have therapeutic implications. Immunotherapy is particularly attractive since ASPH: 1) is a transmembrane protein with high expression on tumor cell surface; 2) expresses at very low levels in normal human tissues; 3) has a defined role in promoting cell proliferation, migration, invasion, and metastasis; 4) high expression confers a poor prognosis characterized by early disease reoccurrence, reduced overall survival, and a highly undifferentiated aggressive phenotype [27, 28].

http://dx.doi.org/10.1016/j.heliyon.2017.e00407

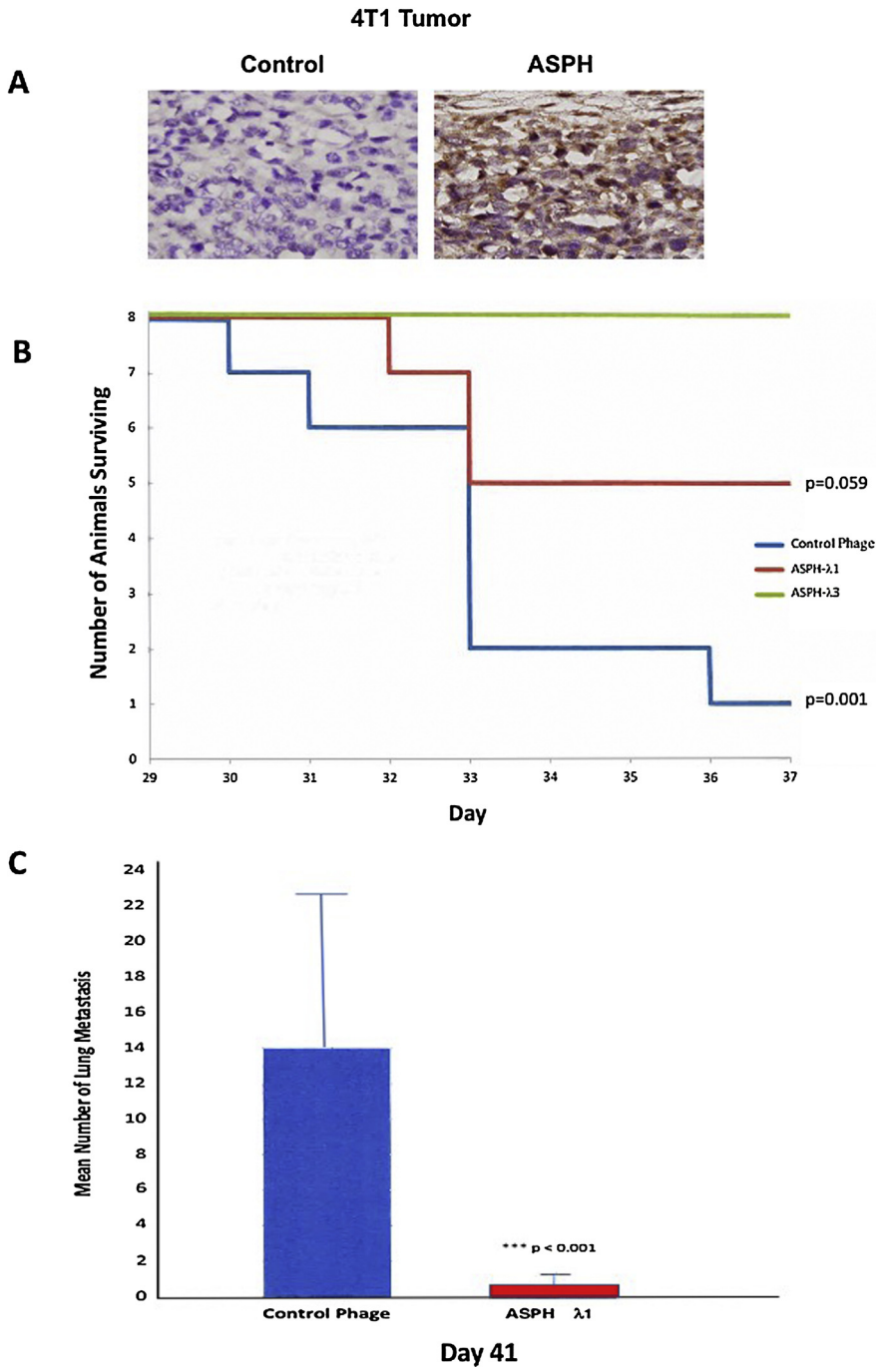

Fig. 9. Demonstration of λ1 and λ3 phage vaccination anti-tumor effects on ASPH expressing murine 4T1 breast carcinomas. (A) Representative example of IHC staining of 4T1 induced breast tumor demonstrating high level ASPH expression in tumor cells using a polyclonal rabbit anti-ASPH primary antibody compared to the rabbit IgG antibody control (1000×). (B) Kaplan-Meier plots demonstrating anti-tumor effects of ASPH- λ1 and ASPH- λ3 vaccines on animal survival with ASPH expressing murine 4T1 breast carcinoma cells implanted into the mammary gland compared to empty phage vector control (N = 8). There was a significant difference (p = 0.001) between control phage immunized mice and mice vaccinated with ASPH- λ3 vaccine. Improvement in animal survival was also suggested

http://dx.doi.org/10.1016/j.heliyon.2017.e00407

There has been increasing interest in bacteriophages as vectors for vaccine delivery [29, 30, 31, 32, 33, 34, 35]. They have high stability and are resistant to enzyme cleavage, high temperatures and wide pH changes. Furthermore, phage vaccines appear non-pathogenic, do not replicate in eukaryotic cells, and lack antibiotic resistance genes. More important, the phage itself performs as a natural adjuvant and may promote enhanced uptake into DCs.

The murine ASPH expressing BNL cell line produces rapid growth when implanted subcutaneously into syngeneic BALB/c mice and inoculated animals may have to be euthanized as early as 4–5 weeks later due to advanced tumors as characterized by large size, and poorly differentiated status [18]. The level of ASPH expression in BNL induced tumors is robust as shown in Fig. 2B. Using this tumor model system, we addressed the question if an immunotherapeutic approach using both a λ1 and λ3 phage ASPH peptide containing vaccine constructs would inhibit HCC growth and progression. We chose the immunization schedule in our study that might mimic a hypothetical clinical situation of proposed use by prophylactic vaccination before a surgical resection of HCC followed by booster doses in an attempt to prevent early disease recurrence and retard the growth and progression of established micro-metastatic disease. This hypothesis assumes that there may be a small number of residual tumor cells following surgery that could be effectively abolished or reduced by a λ phage generated immune response [36, 37, 38].

The λ phage vaccine was highly immunogenic and induced antigen specific CD4+ and CD8+ CTL actively in splenocytes derived from tumor bearing mice. Previous studies using this same syngeneic tumor animal model had demonstrated DCs loaded with ASPH *ex vivo* and used as a vaccine generated, robust antigen specific CD4+ and CD8+ activity; the anti-tumor effect on BNL HCC growth was substantially reduced by CD4+ and CD8+ depletion with specific antibodies [18]. We also observed that λ3 phage vaccination resulted in increased secretion of Th1 (IFNγ and TNF-α and Th2 (IL-4, IL-6 and IL-10) cytokines in the cell culture supernatant of splenocytes derived from immunized mice (Fig. 6). Immunization with λ3 phage particles elicited a lower production of IL-2 from splenocytes compared to controls (Fig. 6A). In this regard, IL-2 is a pro-inflammatory and strong immunoregulatory Th1 type cytokine. It is known that the IL-2 production is

following vaccination with the ASPH-λ1 vaccine construct compared to controlled phage but did not reach statistical significance ($p = 0.59$). There were 8 animals in each group. (C) Reduction in 4T1 murine breast carcinoma cell metastasis from the primary tumor site of growth in the mammary gland to the lung following vaccination with the ASPH-λ1 construct compared to the empty phage construct as a control ($p < 0.001$). Mice ($N = 8$) in both groups were vaccinated s.q. on days 1, 8, 15 and 29 with 1×10^{10} pfu and challenged in the mammary gland on day 20 with 2×10^4 4T1 cells and sacrificed at day 41 and the lungs stained with Bouin's solution and counted for metastases.

http://dx.doi.org/10.1016/j.heliyon.2017.e00407

transient and limited by a negative feedback loop that depends, in part, on other cytokine signals [39]. These observations suggest that IL-2 may be negatively regulated by the secretion of Th2-type cytokines, most notably IL-4 and especially the high level production of IL-10 (3000–4000 pg/ml) found here. It has been previously reported that IL-4 inhibits IL-2 synthesis by CD4+ T cells [40]. In addition, IL-10 has been found to inhibit T cell proliferation and IL-2 production as well [41, 42]. A consistent enhanced secretion Th2 cytokines by splenocytes following λ phage vaccination against ASPH expressing BNL HCC cells was observed as shown in Fig. 6B; the mechanisms for these observations will require further exploration.

However, anti-tumor effects were exhibited *in vivo* since both λ1 and λ3 vaccinations delayed HCC growth and progression as well as improved the overall survival rate (Fig. 3 and Fig. 4). The residual tumor expression of ASPH after vaccination was also examined. Interestingly, the remaining tumor cells still express ASPH as shown in Fig. 7. Such observations imply that additional immunizations may be required to achieve optimal antitumor activity.

The pathological features of the tumors following λ3 vaccinations were informative; the HCCs derived from immunized mice were characterized by extensive necrosis and edema with substantial infiltration of CD3+ and CD8+ lymphocytes (as shown in Fig. 7). In contrast, the BNL induced tumors obtained from the controls lacked edema, necrosis and infiltration of CD3+ and CD8+ T-cells as well as CD45+ mononuclear cells. When tumors derived from both vaccinated and control mice reached a size of approximately 500 mm^3, the animals were euthanized. The gross and histologic findings in the tumor obtained from vaccinated mice were reminiscent of pseudo-progression [43, 44, 45]. The λ3 phage vaccine construct appeared to drive antigen (ASPH) specific T-cells into the tumor parenchyma and produce concomitant tumor necrosis and edema. It would be interesting to perform immunotherapy with the addition of anti-CTL4, and/or PD-1/PD-L1 antibodies [46, 47] to enhance their cytotoxic capacity. Finally, we have not yet evaluated the anti-tumor effects of NK cells in this syngeneic murine HCC model and additional studies will be required.

4. Materials and methods

4.1. Cell lines and culture

The BNL 1ME A.7R.1 (BNL) and 4T1 murine cell lines were purchased from the American Type Tissue Culture Collection (Manassas, VA). Cell lines were maintained in Dulbecco's modified Eagle's medium supplemented with 10% fetal bovine serum (FBS) and 2 mM of L-glutamine and cultivated in a humidified incubator at 37 °C with 5% CO_2.

http://dx.doi.org/10.1016/j.heliyon.2017.e00407

4.2. Recombinant human aspartate-β-hydroxylase protein preparation

The full length human ASPH (GenBank accession No. S83325) was cloned into the EcoRI site of the pcDNA vector (Invitrogen, Carlsbad, CA). Recombinant ASPH protein (rASPH) was produced in a Baculovirus system (Invitrogen) according to manufacturer's instruction [10, 17, 18].

4.3. Construction of bacteriophage λ to display ASPH peptides

We designed a bacteriophage λ system to display ASPH fused at the carboxyl terminus of the capsid protein gpD of λ phage. Due to limitations on the size of the DNA that can be incorporated into viable λ phage, the ASPH sequence was segmented into thirds that would allow for proper display of ASPH peptides on λ head. This work focuses on both the N and C-terminal regions of the ASPH protein, designated as ASPH constructs λ1 and λ3 respectively. Using ASPH specific oligo primers these segments were amplified from the ASPH gene. The oligo sequence of each PCR primer was modified to produce restriction sites for Nhe I and Bssh II enzymes at each end of the amplified ASPH segment. After restriction enzyme digestion, this segment was inserted at the NheI-BsshII site of the 3′ end of a DNA segment encoding GpD under the control of the lac promoter. These constructs were created in donor plasmid pVCDcDL1A, which carries *loxPwt* and *loxP511* sequences. Cre-expressing *E. coli* was transformed with these recombinant plasmids and subsequently infected with recipient λ phage DL1 (λ-DL1) that carried a stuffer DNA segment flanked by loxPwt and loxP511 sites. Recombination occurred *in vivo* at the lox sites and then Ampr cointegrates were formed, which spontaneously lysed the *E. coli* and released the products in culture media. These cointegrates produced recombinant phage that display ASPH peptides fused at the C-terminus of GpD. Recombination with unmodified pVCDcDL3 alone yielded control phage particles without the display of ASPH peptides as described [48].

4.4. Animals, tumor challenge and immunization

Female BALB/c mice aged 6-8-week-old (Charles River Laboratories, Wilmington, MA) were employed. All animal protocols were approved by the Institutional Animal Care and Use Committee of Rhode Island Hospital (Providence, RI). Mice were immunized by injecting 1×10^{10} pfu of phage particles suspended in 100 μL of sterile saline into the base of the tail. The experimental design is shown in Fig. 1. We chose a prophylactic vaccination schedule three times spaced a week apart prior to BNL HCC cells inoculation. The BNL cells (5×10^{6}) were subcutaneously inoculated into the right flank. Booster immunization was continuously administrated every 7–10 days after tumor inoculation. Tumor size was measured

http://dx.doi.org/10.1016/j.heliyon.2017.e00407

using calipers 2–3 times per week, and tumor volume was calculated as $A \times B^2 \times 0.5$ (A, length; B, width). Six to eight weeks after tumor inoculation, mice bearing tumors with the shorter diameter exceeded 10 mm were euthanized according to the requirements of the Animal Welfare Committee of the Rhode Island Hospital (Providence, RI). Whole blood (400 μL) was collected; spleen and tumor tissues were harvested from each animal. Serum samples were collected following centrifugation and stored at −80 °C. Tumors were excised and fixed with 10% formalin for further immunohistochemistry (IHC) analysis. The procedures for establishing the ASPH expressing breast tumors generated by 4T1 cells were performed as described [14].

4.5. Enzyme-linked immunosorbent assays

The following cytokines IFN-γ, IL-2, IL-4, IL-6, TNF-α and IL-10 were measured in cell culture supernatants after 4 days of splenocyte re-stimulation with phage particles and rASPH using murine high sensitivity ELISA kits (eBioscience).

4.6. Isolation and characterization of murine splenocytes

Spleens were excised from immunized or control mice bearing tumors after euthanasia, dispersed using the plunger end from a 3 ml syringe, and then passed through a 70 μm cell strainer. Erythrocytes were lysed with lysis solution buffer (BD Biosciences, San Jose, CA). After isolation, splenocytes were re-stimulated following culture in RPMI-1640 (supplemented with 10% FBS, 1 × non-essential amino acids, 1 × amino acid solution, 100 μM sodium pyruvate, 1 × penicillin-streptomycin and 50 μM 2- mercaptoethanol) with 0.5 μg/ml rASPH and 2×10^8 pfu/ml Phage particles for 4 days, as modified from a previous published protocol [18]. Then 10 ng/ml IL-2 (PeproTech, Rocky Hill, NJ) was added continuously for 2 days after the start of culture. Following a 4-day re-stimulation of splenocytes with phage and rASPH, the supernatants derived from culture media were collected for enzyme-linked immunosorbent assay (ELISA) to measure cytokine secretion. This assay had been previously optimized for DC activation of murine and human antigen specific CD4+ and CD8+ T cell activity as described [49]; it also was previously optimized for T cell activation using DCs pulsed with ASPH containing microparticles in both mice and humans [10, 18]. Density-gradient centrifugation was performed with the re- stimulated splenocytes using Lympholyte M (Cedarlane, Burlington, NC) to remove dead cells. Purified re-stimulated splenocytes were used for further cytotoxicity assay and flow cytometric analysis.

4.7. Cytotoxicity assays

Cytotoxicity assays were performed as previously described [18].

http://dx.doi.org/10.1016/j.heliyon.2017.e00407

4.8. Flow cytometric analysis

The re-stimulated splenocytes were resuspended in phosphate buffered saline (PBS) containing 1% fetal bovine serum (FBS). Cells were incubated with the blocking monoclonal antibody (mAb) 2.4G2 and stained with the indicated mAbs specific for cell surface markers for 20 min on ice. For intracellular staining, cells were fixed with Cytofix/Cytoperm (BD Biosciences) for 20 min, and then stained in 1 × PermWash (BD Biosciences) for 20 min. Washed cells were assessed by a FACS Aria cytometer (BD Biosciences), and the data was analyzed using FlowJo software (Tree Star Inc., Ashland, OR). As a gating strategy, we firstly gated on lymphocytes based on forward scatter (FSC)-area versus side scatter (SSC)-area. Within this population, doublets were excluded by analyzing FSC-height versus FSC-width. Dead cells were also excluded using dead/live stain. For characterization of CD4, CD8 and regulatory T cells, the following conjugated anti– mouse mAbs were used: CD4 (clone GK1.5; eBioscience, San Diego, CA), CD8a (clone 53–6.7; Biolegend, San Diego, CA), TCRβ (clone H57-597; eBioscience), CD25 (clone PC61; Biolegend), FoxP3 (clone FJK-16s; eBioscience), CD154 (clone MR1; eBioscience), CD137 (clone 17B5; eBioscience), and IFN-γ (clone XMG1.2; eBioscience). To exclude the dead cells from the analysis, we used a LIVE/DEAD fixable dead cell stain (Invitrogen). Appropriate isotype controls were included in each analysis.

4.9. Evaluation of tumor-infiltrating lymphocytes

Tumors were excised from the immunized mice 6–8 weeks after inoculation of BNL cells, and formalin-fixed paraffin-embedded sections were prepared. After deparaffinization, antigen retrieval and endogenous peroxidase blocking, immunohistochemical staining was performed using the VECTASTAIN Elite ABC kit (Vector Laboratories, Burlingame, CA) according to the manufacture's protocol. Primary antibodies were diluted at 1:250, 1:400, 1:100 and 1:50 for rabbit polyclonal anti-ASPH antibody, rabbit monoclonal anti-CD3 antibody (SP7; Abcam, Cambridge, MA), rat monoclonal anti-CD8 (eBioscience, San Diego, CA) and CD45 (Abcam, Cambridge, MA). Sections were incubated with primary antibodies at 4 °C overnight, then color development was performed using DAB Peroxidase Substrate (Vector Laboratories) for 60–90 seconds (ASPH, CD3 and CD8). Counterstaining was performed by hematoxylin. The CD3 and CD8 positive T cells were counted per randomly selected 5–10 high-power fields (400×) and CD45 positive cells were counted in 10 fields (1000×) by using Imagesoftware (NIH, Bethesda, MD). We calculated mean number of CD3 and CD8 positive T cells as well as CD45 cells infiltrating the tumor parenchyma from 5 different sections derived from 3–5 tumors.

4.10. Statistical analysis

Statistical analysis was conducted using SPSS software. Quantitative data were presented as means ± SEM. Quantitative data were analyzed by one-way analysis

 http://dx.doi.org/10.1016/j.heliyon.2017.e00407

of variance (ANOVA) (multiple groups) or Student's *t* tests (two groups). IHC scores from different groups were compared by $\chi 2$ test. Survival time was estimated using the Kaplan-Meier method. Difference in median survival time between control and experimental group was examined by log-rank *t* test. A p-value of <0.05 (two-sided) was considered as statistically significant.

Declarations

Author contribution statement

Yoshifumi Iwagami, Michael S. Lebowitz: Conceived and designed the experiments; Performed the experiments; Analyzed and interpreted the data; Wrote the paper.

Sarah Casulli: Performed the experiments; Analyzed and interpreted the data; Wrote the paper.

Katsuya Nagaoka, Miran Kim, Rolf I. Carlson, Kosuke Ogawa, Biswajit Biswas, Solomon Stewart: Performed the experiments; Analyzed and interpreted the data.

Steve Fuller: Conceived and designed the experiments.

Xiaoqun Dong, Hossein Ghanbari, Jack R. Wands: Conceived and designed the experiments; Wrote the paper.

Competing interest statement

The authors declare the following conflicts of interest: Hossein Ghanbari, Steve Fuller, Soloman Stewart and Michael S. Lebowitz are full time employees at Panacea Pharmaceuticals. The other authors declare no conflict of interest.

Funding statement

This work was supported in part from NIH grant CA123544, institutional funds and grant from Panacea Pharmaceuticals.

Additional information

No additional information is available for this paper.

References

[1] World Cancer Report 2014: The Global Economic Burden of Cancer, World Health Organization, 2014.

http://dx.doi.org/10.1016/j.heliyon.2017.e00407

[2] E.C. Lai, S.T. Fan, C.M. Lo, K.M. Chu, C.L. Liu, J. Wong, Hepatic resection for hepatocellular carcinoma. An audit of 343 patients, Ann. Surg. 221 (1995) 291–298.

[3] A. Villanueva, V. Hernandez-Gea, J.M. Llovet, Medical therapies for hepatocellular carcinoma: a critical view of the evidence, Nat. Rev. Gastroenterol. Hepatol. 10 (2013) 34–42.

[4] J.M. Llovet, S. Ricci, V. Mazzaferro, P. Hilgard, E. Gane, J.F. Blanc, A.C. de Oliveira, et al., Sorafenib in advanced hepatocellular carcinoma, N. Engl. J. Med. 359 (2008) 378–390.

[5] J. Bruix, T. Takayama, V. Mazzaferro, G.Y. Chau, J. Yang, M. Kudo, J. Cai, et al., Adjuvant sorafenib for hepatocellular carcinoma after resection or ablation (STORM): a phase 3, randomised, double-blind, placebo-controlled trial, Lancet Oncol. 16 (2015) 1344–1354.

[6] R. Lencioni, J.M. Llovet, G. Han, W.Y. Tak, J. Yang, A. Guglielmi, S.W. Paik, et al., Sorafenib or placebo plus TACE with doxorubicin-eluting beads for intermediate stage HCC: the SPACE trial, J. Hepatol. (2016).

[7] S. Jia, W.J. VanDusen, R.E. Diehl, N.E. Kohl, R.A. Dixon, K.O. Elliston, A. M. Stern, et al., cDNA cloning and expression of bovine aspartyl (asparaginyl) beta-hydroxylase, J. Biol. Chem. 267 (1992) 14322–14327.

[8] L. Lavaissiere, S. Jia, M. Nishiyama, S. de la Monte, A.M. Stern, J.R. Wands, P.A. Friedman, Overexpression of human aspartyl(asparaginyl)beta-hydroxylase in hepatocellular carcinoma and cholangiocarcinoma, J. Clin. Invest. 98 (1996) 1313–1323.

[9] A. Aihara, C.K. Huang, M.J. Olsen, Q. Lin, W. Chung, Q. Tang, X. Dong, et al., A cell-surface beta-hydroxylase is a biomarker and therapeutic target for hepatocellular carcinoma, Hepatology 60 (2014) 1302–1313.

[10] Y. Tomimaru, S. Mishra, H. Safran, K.P. Charpentier, W. Martin, A.S. De Groot, S.H. Gregory, et al., Aspartate-beta-hydroxylase induces epitope-specific T cell responses in hepatocellular carcinoma, Vaccine 33 (2015) 1256–1266.

[11] G.P. Smith, Filamentous fusion phage: novel expression vectors that display cloned antigens on the virion surface, Science 228 (1985) 1315–1317.

[12] A. Gupta, M. Onda, I. Pastan, S. Adhya, V.K. Chaudhary, High-density functional display of proteins on bacteriophage lambda, J. Mol. Biol. 334 (2003) 241–254.

 http://dx.doi.org/10.1016/j.heliyon.2017.e00407

[13] P.S. Sepe, S.A. Lahousse, B. Gemelli, H. Chang, T. Maeda, J.R. Wands, S.M. de la Monte, Role of the aspartyl-asparaginyl-beta-hydroxylase gene in neuroblastoma cell motility, Lab. Invest. 82 (2002) 881–891.

[14] A.C. Gregorio, N.A. Fonseca, V. Moura, M. Lacerda, P. Figueiredo, S. Simoes, S. Dias, et al., Inoculated cell density as a determinant factor of the growth dynamics and metastatic efficiency of a breast cancer murine model, PLoS One 11 (2016) e0165817.

[15] J. Engel, EGF-like domains in extracellular matrix proteins: localized signals for growth and differentiation, FEBS Lett. 251 (1989) 1–7.

[16] Q.P. Wang, W.J. VanDusen, C.J. Petroski, V.M. Garsky, A.M. Stern, P.A. Friedman, Bovine liver aspartyl beta-hydroxylase: purification and characterization, J. Biol. Chem. 266 (1991) 14004–14010.

[17] T. Noda, M. Shimoda, V. Ortiz, A.E. Sirica, J.R. Wands, Immunization with aspartate-beta-hydroxylase-loaded dendritic cells produces antitumor effects in a rat model of intrahepatic cholangiocarcinoma, Hepatology 55 (2012) 86–97.

[18] M. Shimoda, Y. Tomimaru, K.P. Charpentier, H. Safran, R.I. Carlson, J. Wands, Tumor progression-related transmembrane protein aspartate-beta-hydroxylase is a target for immunotherapy of hepatocellular carcinoma, J. Hepatol. 56 (2012) 1129–1135.

[19] N. Ince, S.M. de la Monte, J.R. Wands, Overexpression of human aspartyl (asparaginyl) beta-hydroxylase is associated with malignant transformation, Cancer Res. 60 (2000) 1261–1266.

[20] M.C. Cantarini, S.M. de la Monte, M. Pang, M. Tong, A. D'Errico, F. Trevisani, J.R. Wands, Aspartyl-asparagyl beta hydroxylase over-expression in human hepatoma is linked to activation of insulin-like growth factor and notch signaling mechanisms, Hepatology 44 (2006) 446–457.

[21] C.K. Huang, Y. Iwagami, A. Aihara, W. Chung, S. de la Monte, J.M. Thomas, M. Olsen, et al., Anti-tumor effects of second generation beta-hydroxylase inhibitors on cholangiocarcinoma development and progression, PLoS One 11 (2016) e0150336.

[22] Y. Iwagami, C.K. Huang, M.J. Olsen, J.M. Thomas, G. Jang, M. Kim, Q. Lin, et al., Aspartate beta-hydroxylase modulates cellular senescence via glycogen synthase kinase 3beta in hepatocellular carcinoma, Hepatology (2015).

[23] X. Dong, Q. Lin, A. Aihara, Y. Li, C.K. Huang, W. Chung, Q. Tang, et al., Aspartate beta-hydroxylase expression promotes a malignant pancreatic cellular phenotype, Oncotarget 6 (2015) 1231–1248.

 http://dx.doi.org/10.1016/j.heliyon.2017.e00407

[24] Y. Tomimaru, H. Koga, T.H. Shin, C.Q. Xu, J.R. Wands, M. Kim, The SxxSS motif of T-cell factor-4 isoforms modulates Wnt/beta-catenin signal activation in hepatocellular carcinoma cells, Cancer Lett. 336 (2013) 359–369.

[25] S.M. de la Monte, M. Tong, R.I. Carlson, J.J. Carter, L. Longato, E. Silbermann, J.R. Wands, Ethanol inhibition of aspartyl-asparaginyl-beta-hydroxylase in fetal alcohol spectrum disorder: potential link to the impairments in central nervous system neuronal migration, Alcohol 43 (2009) 225–240.

[26] W. Chung, M. Kim, S. de la Monte, L. Longato, R. Carlson, B.L. Slagle, X. Dong, et al., Activation of signal transduction pathways during hepatic oncogenesis, Cancer Lett. 370 (2016) 1–9.

[27] T. Maeda, K. Taguchi, S. Aishima, M. Shimada, D. Hintz, N. Larusso, G. Gores, et al., Clinicopathological correlates of aspartyl (asparaginyl) beta-hydroxylase over-expression in cholangiocarcinoma, Cancer Detect. Prev. 28 (2004) 313–318.

[28] K. Wang, J. Liu, Z.L. Yan, J. Li, L.H. Shi, W.M. Cong, Y. Xia, et al., Overexpression of aspartyl-(asparaginyl)-beta-hydroxylase in hepatocellular carcinoma is associated with worse surgical outcome, Hepatology 52 (2010) 164–173.

[29] J.R. Clark, J.B. March, Bacteriophage-mediated nucleic acid immunisation, FEMS Immunol. Med. Microbiol. 40 (2004) 21–26.

[30] J. Fang, G. Wang, Q. Yang, J. Song, Y. Wang, L. Wang, The potential of phage display virions expressing malignant tumor specific antigen MAGE-A1 epitope in murine model, Vaccine 23 (2005) 4860–4866.

[31] J. Gao, Z. Liu, M. Huang, X. Li, Z. Wang, T7 phage displaying latent membrane protein 1 of Epstein-Barr virus elicits humoral and cellular immune responses in rats, Acta Virol. 55 (2011) 117–121.

[32] J. Gao, Y. Wang, Z. Liu, Z. Wang, Phage display and its application in vaccine design, Ann. Microbiol. 60 (2010) 13–19.

[33] A. Ghaemi, H. Soleimanjahi, P. Gill, Z. Hassan, S.R. Jahromi, F. Roohvand, Recombinant lambda-phage nanobioparticles for tumor therapy in mice models, Genet. Vaccines Ther. 8 (2010) 3.

[34] J.B. March, J.R. Clark, C.D. Jepson, Genetic immunisation against hepatitis B using whole bacteriophage lambda particles, Vaccine 22 (2004) 1666–1671.

 http://dx.doi.org/10.1016/j.heliyon.2017.e00407

[35] A.W. Purcell, J. McCluskey, J. Rossjohn, More than one reason to rethink the use of peptides in vaccine design, Nat. Rev. Drug Discov. 6 (2007) 404–414.

[36] T.M. Kundig, G. Senti, G. Schnetzler, C. Wolf, B.M. Prinz Vavricka, A. Fulurija, F. Hennecke, et al., Der p 1 peptide on virus-like particles is safe and highly immunogenic in healthy adults, J. Allergy Clin. Immunol. 117 (2006) 1470–1476.

[37] R. Sartorius, P. Pisu, L. D'Apice, L. Pizzella, C. Romano, G. Cortese, A. Giorgini, et al., The use of filamentous bacteriophage fd to deliver MAGE-A10 or MAGE-A3HLA-A2-restricted peptides and to induce strong antitumor CTL responses, J. Immunol. 180 (2008) 3719–3728.

[38] L. Zhikui, G. Changcun, N. Yongzhan, H. Fengtian, R. Xingling, L. Shujun, H. Zheyi, et al., Screening and identification of recombinant anti-idiotype antibodies against gastric cancer and colon cancer monoclonal antibodies by a phage-displayed single-chain variable fragment library, J. Biomol. Screen. 15 (2010) 308–313.

[39] A.V. Villarino, C.M. Tato, J.S. Stumhofer, Z. Yao, Y.K. Cui, L. Hennighausen, J.J. O'Shea, T. et al. Helper, cell IL-2 production is limited by negative feedback and STAT-dependent cytokine signals, J. Exp. Med. 204 (2007) 65–71.

[40] O.M. Martinez, R.S. Gibbons, M.R. Garovoy, F.R. Aronson, IL-4 inhibits IL-2 receptor expression and IL-2-dependent proliferation of human T cells, J. Immunol. 144 (1990) 2211–2215.

[41] K. Taga, G. Tosato, IL-10 inhibits human T cell proliferation and IL-2 production, J. Immunol. 148 (1992) 1143–1148.

[42] K.N. Couper, D.G. Blount, E.M. Riley, IL-10: the master regulator of immunity to infection, J. Immunol. 180 (2008) 5771–5777.

[43] G. Finocchiaro, S. Pellegatta, Perspectives for immunotherapy in glioblastoma treatment, Curr. Opin. Oncol. 26 (2014) 608–614.

[44] R.Y. Huang, M.R. Neagu, D.A. Reardon, P.Y. Wen, Pitfalls in the neuroimaging of glioblastoma in the era of antiangiogenic and immuno/targeted therapy – detecting illusive disease, defining response, Front. Neurol. 6 (2015) 33.

[45] C. Kamiya-Matsuoka, M.R. Gilbert, Treating recurrent glioblastoma: an update, CNS Oncol. 4 (2015) 91–104.

[46] M.D. Hellmann, C.F. Friedman, J.D. Wolchok, Combinatorial cancer immunotherapies, Adv. Immunol. 130 (2016) 251–277.

 http://dx.doi.org/10.1016/j.heliyon.2017.e00407

[47] W. Zou, J.D. Wolchok, L. Chen, PD-L1 (B7-H1) and PD-1 pathway blockade for cancer therapy: Mechanisms, response biomarkers, and combinations, Sci. Transl. Med. 8 (2016) 328rv324.

[48] E.F.F.J. Sambrook, T. Maniatis, Molecular Cloning, Second Edition, Cold Spring Harbor Laboratory Press, New York, 1989.

[49] J.M. Moser, E.R. Sassano, C. Leistritz del, J.M. Eatrides, S. Phogat, W. Koff, D.R. Drake 3rd, Optimization of a dendritic cell-based assay for the in vitro priming of naive human CD4+ T cells, J. Immunol. Methods 353 (2010) 8–19.